Application Note

Cell Analysis

Agilent

Trusted Answers

Rapid Bioenergetic Functional Screening of Anticancer Drug Candidates

Using the Agilent Seahorse XF Real-Time ATP rate assay to detect metabolic modulation

Authors

Yoonseok Kam, Lisa Winer, and Natalia Romero
Agilent Technologies, Inc.

Abstract

The regulation of cellular bioenergetics is recognized as a key driver of cancer cell proliferation. Identifying key pathways that modulate bioenergetic metabolism is a promising strategy for developing novel therapeutic targets for cancer treatment. Quantifying the rate of adenosine triphosphate (ATP) production from glycolysis and mitochondria simultaneously in live cells offers an important view into cellular bioenergetics. A new workflow for rapid functional screening of agents modulating cancer cell metabolism is applied using the Agilent Seahorse XF Real-Time ATP rate assay combined with up-to-date data analysis software. This application note introduces how informative the XF Real-Time ATP rate assay data is in selecting metabolic modulators and evaluating drug potency. A workflow of anticancer drug screening with a kinase inhibitor library is also demonstrated. This workflow can be used to identify drug compounds targeting cancer cell metabolism or druggable targets that impact mitochondrial and glycolytic metabolism.

Introduction

Cancer cells go through metabolic reprogramming during tumor initiation and through cancer progression. There has been significant progress in finding therapeutic targets to exploit metabolic vulnerabilities in cancer cells.[1] In addition, a better understanding of cancer cell metabolism can provide valuable information about the harsh tumor microenvironment, which can profoundly impact the efficacy of emerging immune therapies for solid tumors.[2,3] Demand is growing for time-efficient and robust analytic tools to explore drug targets and genes that modulate cancer cell metabolism.

The XF Real-Time ATP rate assay quantifies basal rates of ATP production from glycolysis and mitochondrial respiration simultaneously. It provides a quantitative characterization of the energetic phenotype of the cells by using ATP production rate as the universal unit to quantify bioenergetic activity. The assay is designed to measure the real-time oxygen consumption rate as well as proton efflux rate of cells with the sequential injection of oligomycin and a mix of rotenone and antimycin A. It allows the calculation of multiple cellular bioenergetic parameters, including (1) mitochondrial ATP production rate (mitoATP rate), (2) glycolytic ATP production rate (glycoATP rate), (3) total ATP production rate (total ATP rate), and (4) XF ATP rate index from a single sample and assay.[4]

The XF Real-Time ATP rate assay represents a valuable tool to screen and investigate candidates for modulating cellular bioenergetic metabolism with multiple benefits as an entry-point assay.

First, the assay provides a sensitive and direct method to detect shifts in basal metabolic phenotype. Because this assay simultaneously measures ATP production from both main bioenergetic pathways, it can quickly identify switches in carbon source usage between mitochondrial respiration and glycolysis in real time. Moreover, by exploiting a common unit of ATP production rate for the two metabolic activities, the metabolic shifts can be quantitatively assessed either by the portion (% glycolysis versus % oxidative phosphorylation) or by the ratio (ATP Rate Index) between both parameters.

Second, this real-time analysis can identify changes in cellular metabolic phenotype that cannot be detected by the widely used measurement of intracellular ATP concentration using fluorescent or luminescent probes. In living cells, intracellular ATP concentration is highly regulated and maintained at a steady state level by adjusting the rates of ATP production and consumption. In other words, cells increase or decrease ATP production by responding to the change in ATP consumption required to perform any cellular function or vice versa. Since significant changes in cellular ATP levels indicate the occurrence of catastrophic events, they are only suited for assessing cell viability.[5,6] In contrast, the real-time measurement of ATP production rate using the XF Real-Time ATP rate assay can measure changes in total cellular energy production metabolism. Those changes can be used to evaluate cellular function (such as activation, differentiation, etc.), as well as to distinguish impacts on the individual bioenergetic pathways, even without significant effect in cell viability.

Third, since it measures basal metabolic rates, the assay only requires two sequential injections of reagents that have a wide range of optimal concentrations. There is no additional reagent optimization step. This advantage simplifies the assay workflow, particularly when screening mitochondrial dysfunction in multiple cell lines or cells with genetic modifications.

Finally, the customized software tools available for the assay can rapidly deliver quantitative measurements of metabolic interference caused by chemical stimulation or genetic modification, including screening and dose-response analysis capabilities.

Experimental

XF Real-Time ATP Rate Assay

The ATP production rates were measured as described in the XF Real-Time ATP Rate Assay User Guide.[7]

A549 (ATCC) and PC-9 (ECACC) cells were cultured in RPMI 1640 (Gibco) supplemented with 2 mM GlutaMax (Gibco) and 10% fetal bovine serum (FBS, HyClone). Cells were seeded in Agilent Seahorse XF Pro M cell culture microplates at a density of 1×10^4 cells per well and cultured overnight. On the day of assay, the media change with the Seahorse XF RPMI medium, pH 7.4 supplemented with 10 mM glucose, 1 mM pyruvate and 2 mM glutamine, cells were incubated for 1 hour without CO_2 at 37 °C in the presence or absence of CB-839 or BAY-876 at 1 µM. After the assay, cells were then counted for data normalization using the BioTek Cytation 1 cell imaging multimode reader and the Agilent Seahorse XF Imaging and Normalization System. All key parameters and graphs were generated using Seahorse Analytics.

The Agilent products required to run XF Real-Time ATP rate assay for screening and dose response studies are listed in Table 1. For a full list of all medium types and our recommendation for each assay kit, please refer to the Agilent Seahorse XF Media Selection Guide.[8]

Kinase inhibitor library screening

THP-1 and PBMC cells were cultured in RPMI 1640 (part number A1049101, Gibco) supplemented with 10% FBS and β-mercaptoethanol, and Immunocult-XF T Cell Expansion Medium (part number 10981, STEMCELL Technologies) respectively. Cells were resuspended in XF RPMI pH 7.4 Assay Media (Agilent) supplemented with 10 mM glucose, 1 mM pyruvate, and 2 mM glutamine, and seeded on Agilent Seahorse XFe96/XF Pro PDL Plates at 2×10^5 cells/well. Cells were incubated in the presence of 1 µM or 10 µM of 80 different kinase inhibitors (SCREEN-WELL Kinase Inhibitor library, part number BML-2832, Enzo Life Sciences) for 1 hour before each assay, while the vehicle control group was incubated in the presence of 0.1% DMSO.

Table 1. Key products required for XF Real-Time ATP rate assay for screening and dose-response analysis.

Item	Product No.
Agilent Seahorse XF Pro analyzer with XF Discovery license	S7855A
Agilent Seahorse XF Real-Time ATP Rate Assay Kit	103592-100
Agilent Seahorse XF Pro M FluxPak, 18 assays*	103775-100
Agilent Seahorse XF Pro M FluxPak Mini, 6 assays*	103777-100
Agilent Seahorse XF Pro M Cell Culture Microplate**	103774-100
Agilent Seahorse XFe96/XF Pro PDL Plates†	103799-100
Agilent Seahorse XF DMEM medium pH 7.4	103575-100
Agilent Seahorse XF RPMI medium pH 7.4	103576-100
Agilent Seahorse XF 1.0 M Glucose solution	103577-100
Agilent Seahorse XF 100 mM Pyruvate solution	103578-100
Agilent Seahorse XF 200 mM Glutamine solution	103579-100

* Part numbers 103775-100 and 103777-100 contain Agilent Seahorse XF sensor cartridges and XF Pro M cell culture plates.

** Part number 103774-100 does not contain XF sensor cartridges, which are also required to perform XF assays. This part number is only needed when extra plates are required for optimizing seeding density.

† Part number 103799-100 does not contain XF sensor cartridges. This part number is only needed when nonadherent blood cancer cells or immune cells are present.

Automated assay setup by using Agilent Bravo liquid handler

The Agilent Bravo liquid handler was used to streamline assay preparation. For all assays, cell washing was performed using the Bravo, leaving a final volume of 100 µL per well in preparation for addition of 100 µL of 2x pretreatment solution. For a library screening, the Bravo was used to prepare and transfer the compounds to the cell plate following plate washing. Labware used is described in the Bravo Seahorse Assay Workbench User Guide.[9] The cell washing protocol is a modification of the protocol included with the Bravo Workflow for Seahorse XFe96 Sample Preparation.[10] Serial dilutions and compound library dilutions were performed in a 96-well reservoir to allow transfer of pretreatment solution in a single step. Injection ports were loaded manually, but this step may also be performed using the Bravo if desired.

CellTiter-Glo Assay

To measure the total ATP level, A549 or PC-9 cells were seeded in conventional white 96-well plates (Greiner) at 2×10^4 cells. The total ATP level was measured with the CellTiter-Glo (Promega) kit according to the manufacturer's manual after an exposure to metabolic modulators for 1 hour.

Results and discussion

Real-time quantification of bioenergetic phenotype changes

As discussed above, the measurement of intracellular ATP level or amount is used frequently to assess cell viability. In contrast, the XF Real-Time ATP rate assay provides more information about cellular metabolic phenotype than the static amount of ATP under non- or sub-lethal conditions.

To demonstrate the sensitivity of the method for the detection of metabolic changes that do not affect intracellular ATP levels, we compare the results obtained when A549 and PC-9, two non-small cell lung cancer cell lines, were exposed for 1 hour to two metabolic suppressors: CB-839, a glutamine synthase inhibitor (Selleck Chemicals) and BAY-876, a Glut1 glucose transporter inhibitor (Selleck Chemicals).

Figure 1A shows the changes in intracellular ATP level measured after the indicated treatments, demonstrating that none of the inhibitors cause significant changes in cell viability of either cell line tested during the duration of the treatment. Similar results were observed when total ATP production rate was measured, with only a small decrease in ATP production rate observed after cells were exposed to CB-839 (Figure 1B). In contrast, when mitochondrial and glycolytic ATP production rates were analyzed separately, a significant decrease was observed after CB-839 and BAY-876 exposure, respectively, as the reciprocal metabolic pathways were upregulated to compensate for the inhibitory effect (Figure 1C and D). As a result, in both cell lines, the treatment with the metabolic inhibitors induced a drastic switch in the cell metabolic phenotype. CB-839 shifted cells to a more glycolytic phenotype and BAY-876 to a more aerobic phenotype (Figure 1E), while the total production rates remained almost constant (Figure 1B).

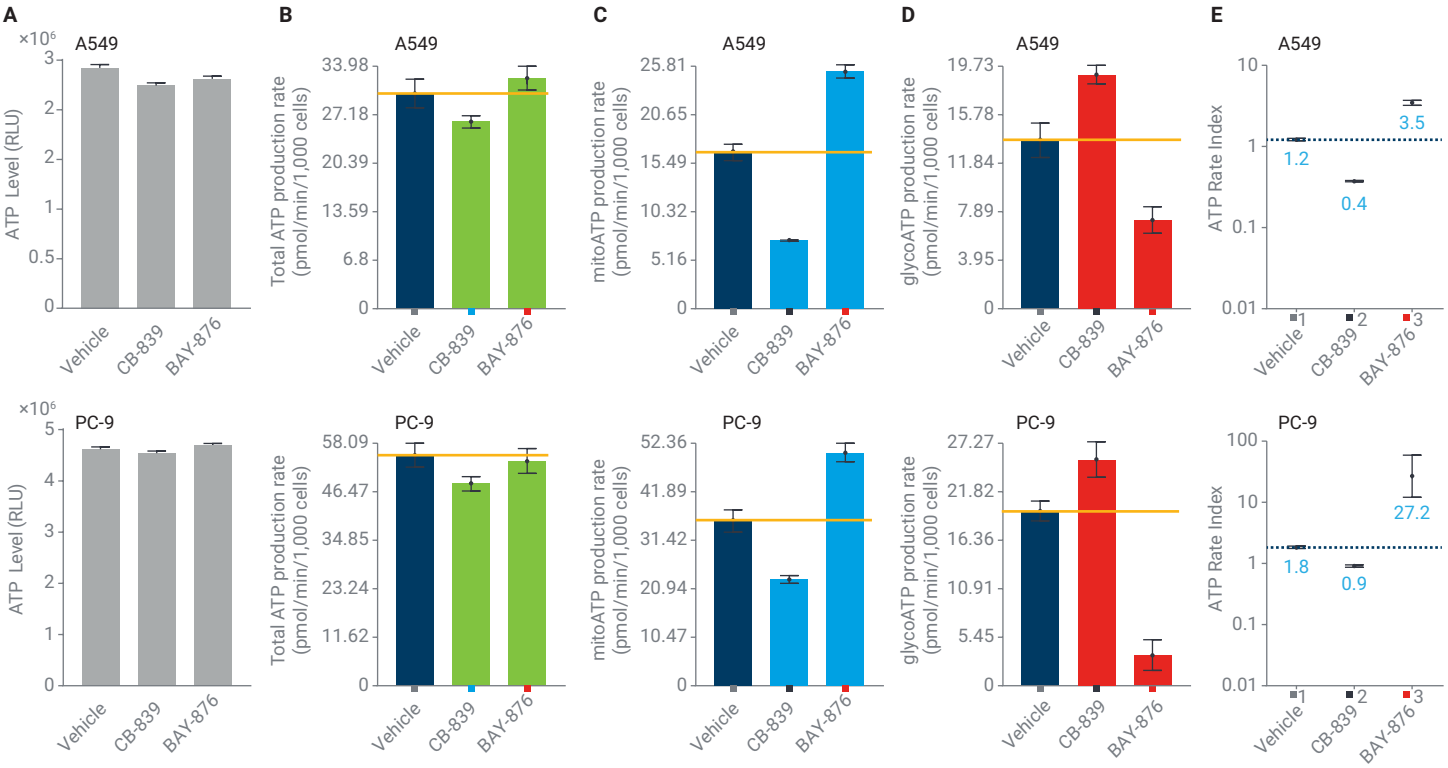

Figure 1. Detection of mitochondrial and glycolytic modulators using the XF Real-Time ATP rate assay. A549 and PC-9 cells were pretreated with the vehicle control (0.1% DMSO), 1 µM CB-839, or 1 µM BAY-876 for 1 hour and analyzed for the static intracellular ATP level (A) and the ATP production rates (B to E). (A) Intracellular ATP concentration measured by CellTiter-Glo. (B) Total ATP production rates. (C) Mitochondrial ATP production rate. (D) Glycolytic ATP production rate. (E) ATP Rate Index. (n = 6, mean ±SD).

In addition, besides monitoring the metabolic phenotype shift caused by inhibitors, the change in the pathway-specific ATP production rate can be quantitatively compared and used to evaluate cell susceptibility to different drugs. The CB-839-caused decrease in the mitoATP production rate and the ATP Rate Index for A549 were bigger than for PC-9 (Figures 1C and 1E). In contrast, PC-9 cells showed a higher reduction of glycoATP production rate in response to BAY-876 and a more significant shift in the ATP Rate Index than A549 (Figures 1D and 1E).

These differences in susceptibility can be more clearly evaluated performing dose-response assays (Figure 2). The dose-response studies of changes in mitoATP rates in response to CB-839 treatment showed >50-fold lower IC_{50} in A549 than PC-9 (Figure 2A). In contrast, IC_{50} of glycoATP rate for BAY-876 was more than eightfold higher for A549 than PC-9 (Figure 2B).

Anticancer metabolic modulator screening

As a simple but robust metabolic phenotype assay, the XF Real-Time ATP rate assay is highly suitable for screening and evaluation of drug potency of metabolic-target drug candidates. As an example, we used a library of kinase inhibitors for screening of cancer cell-specific mitochondrial modulators. The workflow used is illustrated in Figure 3. Briefly, 80 kinase inhibitors from the SCREEN-WELL Kinase inhibitor library (Enzo Life Sciences) were evaluated for metabolic interference in THP-1 cells, an acute monocytic leukemia cell line and peripheral blood mononuclear cells (PBMCs), a non-cancer cell control group. We compared the inhibitory effect on the cell energy metabolism between them and selected inhibitors which showed distinctive effects most significantly. The data from three independent screening replicate assays were combined using the Project tool, a multi-file analysis function in Seahorse Analytics software that helps identify drug candidates that show differential responses in THP-1 and PBMC. In addition, the potency of the selected compounds was further evaluated by comparing the dose responses in both cell types.

All the data analysis was performed using Seahorse Analytics software, which provides ATP production rate workflows that streamline data interpretation for screening compounds and dose-response experiments in early drug discovery.

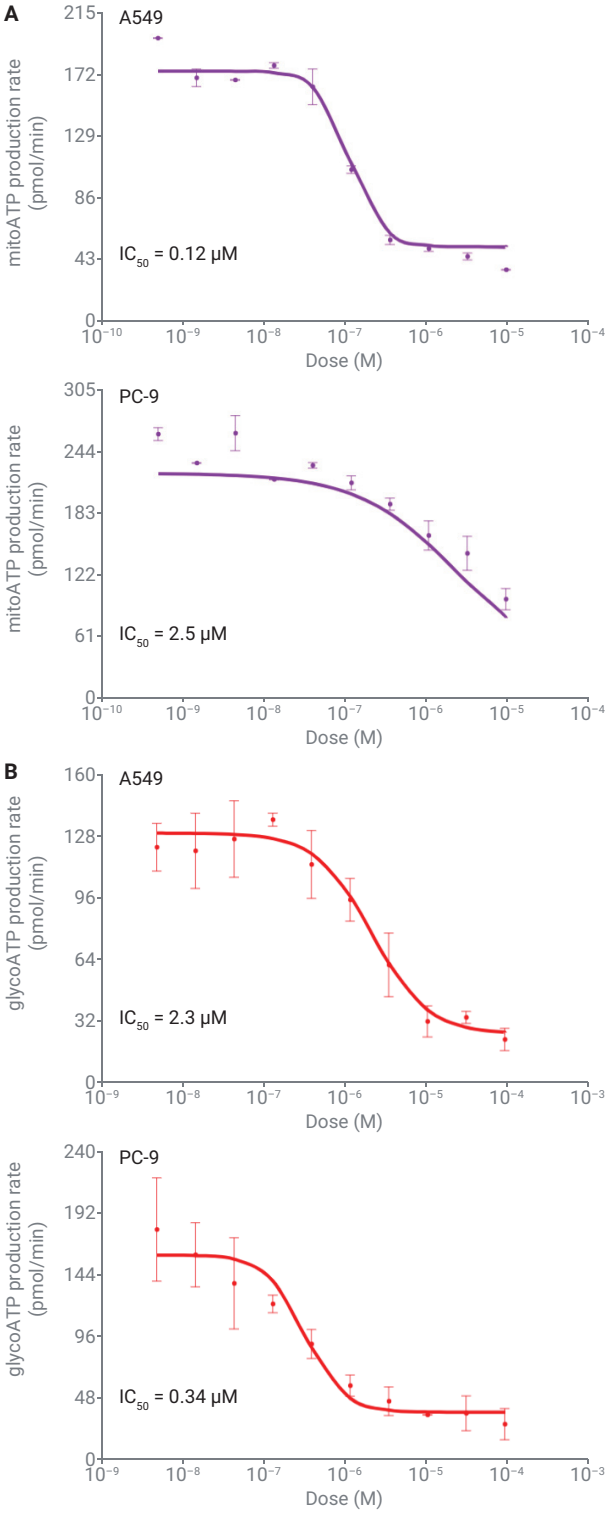

Figure 2. Comparison of susceptibility to the metabolic suppressors between A549 and PC-9 cell lines. A549 and PC-9 cells were pretreated with CB-839 or BAY-876 for 1 hour before the Agilent XF Real-Time ATP rate assay at various concentrations, as indicated. The IC_{50} values were assessed by XF ATP Rate Dose widgets in Agilent Seahorse Analytics. (A) Dose responses of mitoATP rate to CB-839. (B) Dose response of glycoATP rate to BAY-876. (n = 4, mean ±SD).

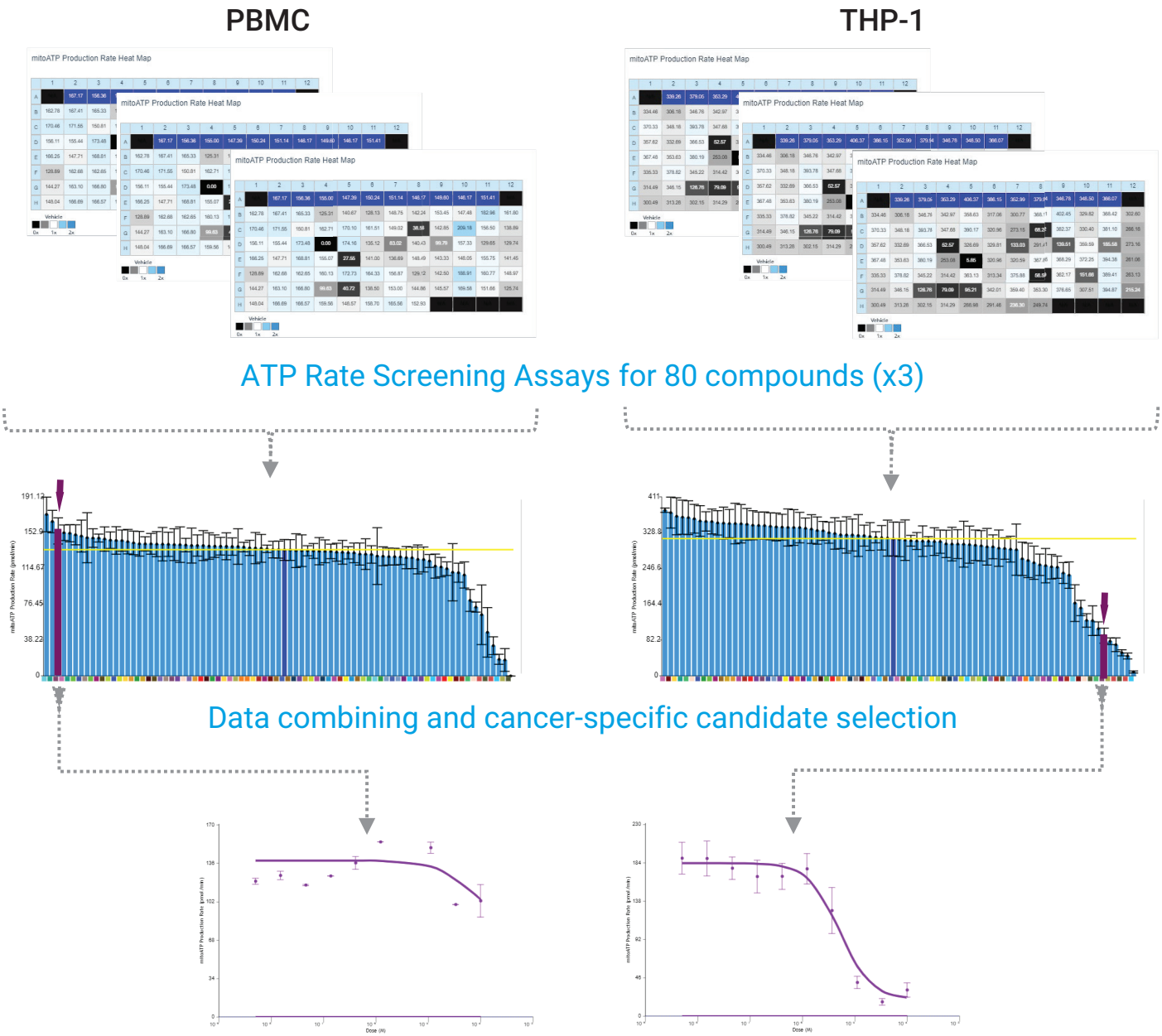

Figure 3. Proposed workflow for screening anticancer drugs targeting cellular metabolism. The effect of compounds on experimental cells (THP-1) and control cells (PBMC) were evaluated by multiple independent XF Real-Time ATP rate assays for each cell type. The replicate assays were combined and compared according to the modulator ranks in Agilent Seahorse Analytics. The drug potency was further analyzed by dose-response studies to select metabolic modulators specific to THP-1 target cells.

Figure 4 shows representative data from the three repeated screening assay results obtained in THP-1 cells. The up- and down-regulation of the ATP production rates by each compound can be represented in various graphical formats, including bar charts and heat maps, so users can quickly identify the most potent metabolic modulators.

In addition, the ATP Rate Index (calculated as the ratio between mitoATP production rate and glycoATP production rate) plot enables the detection of drugs or conditions that cause a significant metabolic shift toward mitochondrial (increase in the index) or glycolytic phenotype (decrease in the index) displayed or exported as spreadsheet for further analysis.

Figure 4. Screening of kinase inhibitors disturbing cellular energy metabolism in cancer cells. THP-1 cells were exposed to various kinase inhibitors (n = 80) for 1 hour before an Agilent Seahorse XF Real-Time ATP rate assay. (A) The effects on the mitochondrial, glycolytic, and total ATP production rates were compared. (B) The energy phenotype shifts induced by the kinase inhibitors were compared using the ATP Rate Index.

In addition, the average combined data of the different output parameters from the replicate assays can be sorted by ascending or descending magnitude, allowing ranking of the kinase inhibitors by the impact of any parameters measured. As shown in Figure 5, when mitoATP rates obtained were sorted by descending order, some kinase inhibitors significantly suppressed the mitoATP production rate in THP-1 cells (Figure 5A), while a smaller number of inhibitors appeared to inhibit mitoATP rates effectively in PBMC (Figure 5B). Several inhibitors were selected after comparing the effects on the mitoATP production rate and ATP Rate Index. For example, SU1498 is one of the compounds that shows the strongest inhibition in mitoATP production in THP-1 cells with almost no effect in PBMC, showing high specificity for the cancer cell type. U0126 showed a moderate effect on the mitoATP rate but also high specificity for THP-1 cells. In contrast, AG-879 was effective on both cell types and slightly more potent in PBMC. Figure 5C shows the datasheet view of mitoATP rates exported from the sorted graph in Seahorse Analytics.

SU1498 is known to inhibit the VEGFR2 receptor and related signaling and induce mitochondrial dysfunction.[11,12] An MEK inhibitor, U0126, was proposed as a potential antileukemia agent and also was reported to inhibit mitochondrial function and induce metabolic phenotype shift to aerobic glycolysis in a MEK-independent manner.[13,14] An ErbB2 kinase inhibitor, AG-879, was reported to induce cancer cell apoptosis, but the effect on mitochondrial metabolism has not been well studied. Indeed, it was reported to suppress Glut1 activity at high concentrations.[15]

The potency of those three drugs was evaluated by performing dose-response studies (Figure 6). As expected, there was no significant difference in susceptibility between THP-1 and PBMC to AG-879. In contrast, SU1398 and U0126 effectively inhibited mitochondrial respiration only in THP-1 cells. All three drugs induce a metabolic shift with a reciprocal increase in glycolysis activity and without significant effect on cell viability after short-term incubation.

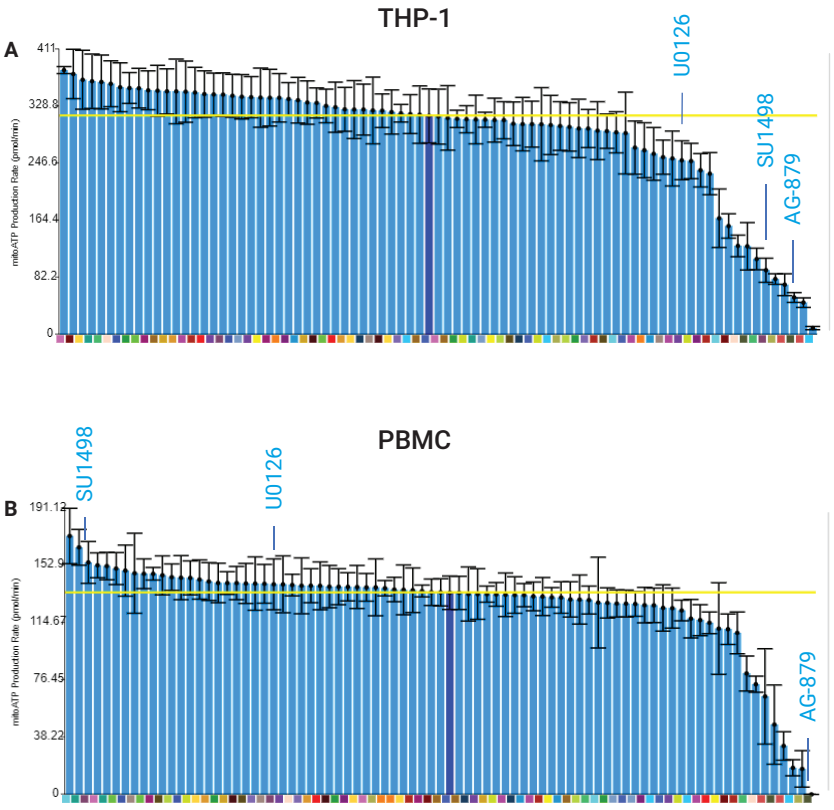

C

THP-1

Group	Value	SEM
Genistein	381.0	5.3
Y-27632 dihydrochloride	375.3	35.7
Lavendustin C	366.9	42.5
Olomoucine, iso-	364.9	39.2
Indirubin	363.8	38.9
HB02II	361.2	33.1
AG-1288	358.2	35.3
HA-1004 HCl	355.1	22.3
LFM-A13	354.8	28.6
Olomoucine, N9-isopropyl-	353.8	28.0
2-Aminopurine	351.2	36.8
Tubastatin analog	350.3	32.6
Tyrphostin 51	350.2	46.6
Apigenin	349.8	44.1
SC-514	348.6	36.4
Tyrphostin 46	346.5	33.3
Tricirbine	345.9	30.6
AG-370	345.7	31.5
ZM 336372	344.0	30.9
DRB	342.5	32.1
HA-100772HCl	342.1	25.7
HNMPA	341.4	42.6
Lavendustin A	341.1	40.9
Olomoucine	341.0	34.8
AG-1296	339.3	23.7
SP600125	337.6	33.0
AG-490	334.2	31.3
Quercetin 2H2O	333.7	21.6
Tyrphostin 47	329.3	24.1
5-Iodotubercidin	327.5	36.2
SB-202190	324.3	31.8
SB203580	324.2	41.9
Sphingosine, D-erythro	324.1	36.6
Daidzein	322.8	48.1
AG-126	322.5	24.2
RMS-257	320.6	31.8
Tyrphostin 25	318.8	12.6
RMS-259	317.6	28.1
AG-825	316.8	41.5
Vehicle	315.3	10.7
Piceatannol	314.1	39.6
Rapamycin	312.0	46.5
Ionic acid	310.8	12.4
ML-7	310.2	19.4
Tyrphostin 23	309.7	35.2
Wortmannin	309.5	10.8
Palmitoylcarnitine chloride	308.9	31.6
Tyrphostin 1	308.8	26.7
TYRPHOSTIN AG 1478	303.7	31.4
Indirubin-3'-monoxime	303.2	38.5
H-8 72HCl	303.1	32.9
BMS-265	302.9	32.7
H-9 HCl	301.8	42.6
LY 294002	300.4	35.0
PP2	299.1	34.9
PD-98059	296.9	42.3
(R)-Roscovitine	296.8	27.4
H-7 2HCl	295.6	41.7
SU4312	293.0	24.9
PKC-412	291.2	29.5
Kenpaullone	290.2	58.9
Staurosporine	289.2	38.3
RG-14620	285.4	39.6
Hypericin (native)	260.2	27.9
PP1	255.4	24.6
ML-7 HCl	253.7	39.5
U-0126	250.3	28.0
AG-494	249.8	25.3
TYRPHOSTIN AG 1295	236.6	24.0
KN-62	233.2	30.4
Rottlerin	167.5	42.1
H-89 2HCl	158.2	17.5
GF 109203X	127.7	15.5
ZM 449829	127.1	14.0
Ro 31-8220 mesylate	108.7	15.5
SU1498	92.6	17.2
BAY 11-7082	79.9	7.7
Tyrphostin 9	71.8	15.7
AG-879	53.5	7.2
GR0574	46.0	6.7
KN-93	9.3	2.3

PBMC

Group	Value	SEM
PKC-412	172.6	18.5
Tyrphostin 23	165.0	11.9
SU1498	154.9	13.9
Genistein	153.1	8.4
Olomoucine, iso-	152.6	9.2
Tyrphostin 47	150.9	10.7
AG-1288	149.5	17.1
PP1	147.7	26.8
LFM-A13	147.4	9.9
Lavendustin A	147.4	4.2
SU4312	146.4	13.0
Tyrphostin 1	145.1	8.9
ZM 336372	144.8	14.7
RMS-265	144.6	11.3
Lavendustin C	143.6	13.2
SB-202190	142.3	12.6
HA-1004 HCl	141.3	13.2
AG-490	141.2	7.5
Quercetin 2H2O	141.2	11.2
TYRPHOSTIN AG 1478	140.9	13.4
(R)-Roscovitine	140.9	17.8
Daidzein	140.7	13.0
AG-370	140.4	17.0
U-0126	140.3	19.1
HB02II	139.9	7.2
Tyrphostin 25	139.4	18.7
Tyrphostin 51	139.4	11.3
Tyrphostin 46	139.3	16.0
AG-126	138.8	14.1
PD-98059	138.8	12.0
AG-1296	138.6	9.4
SB203580	138.5	14.4
Piceatannol	138.3	9.2
LY 294002	138.3	18.9
Olomoucine	137.8	5.1
RG-14620	136.9	8.2
RMS-257	136.7	16.8
SC-514	136.3	14.9
Olomoucine, N9-isopropyl-	135.9	4.0
Y-27632 dihydrochloride	135.1	8.8
Rapamycin	135.0	9.1
Vehicle	134.7	11.2
2-Aminopurine	134.7	11.3
Indirubin-3'-monoxime	133.9	18.1
Tricirbine	133.8	16.9
Tubastatin analog	133.8	5.4
AG-494	133.6	7.9
Apigenin	133.4	14.6
Sphingosine, D-erythro	133.2	12.2
SP600125	133.1	7.7
ML-7 HCl	132.3	9.6
KN-62	132.2	12.7
HNMPA	131.7	6.6
Hypericin (native)	131.6	10.5
AG-825	130.2	11.8
PP2	130.1	16.3
Indirubin	129.9	9.4
Rottlerin	128.2	30.4
Ionic acid	127.9	10.1
DRB	127.6	9.1
Kenpaullone	127.5	9.1
Wortmannin	127.2	8.3
TYRPHOSTIN AG 1295	126.4	11.8
BMS-259	126.3	13.5
H-8 72HCl	124.6	15.5
HA-100772HCl	124.4	13.4
ML-9	122.5	7.0
H-9 HCl	117.5	12.9
Staurosporine	116.4	10.3
5-Iodotubercidin	114.2	7.2
Palmitoylcarnitine chloride	110.8	30.6
H-89 2HCl	110.4	10.2
H-7 2HCl	107.5	14.0
Ro 31-8220 mesylate	80.8	11.7
GF 109203X	73.6	5.4
GR0574	65.4	31.9
ZM 449829	46.6	26.5
Tyrphostin 9	32.4	9.5
KN-93	17.8	5.4
BAY 11-7082	17.1	12.2
AG-879	0.0	0.0

Figure 5. Identification of THP-1 selective antimitochondrial compounds. The inhibitors were ranked by the impact on the mitoATP rate of THP-1 (A) and PBMC (B). Each sorted data set was exported to a Microsoft Excel spreadsheet file in Agilent Seahorse Analytics, and the three compounds are highlighted (C). (n = 3, mean ±SEM).

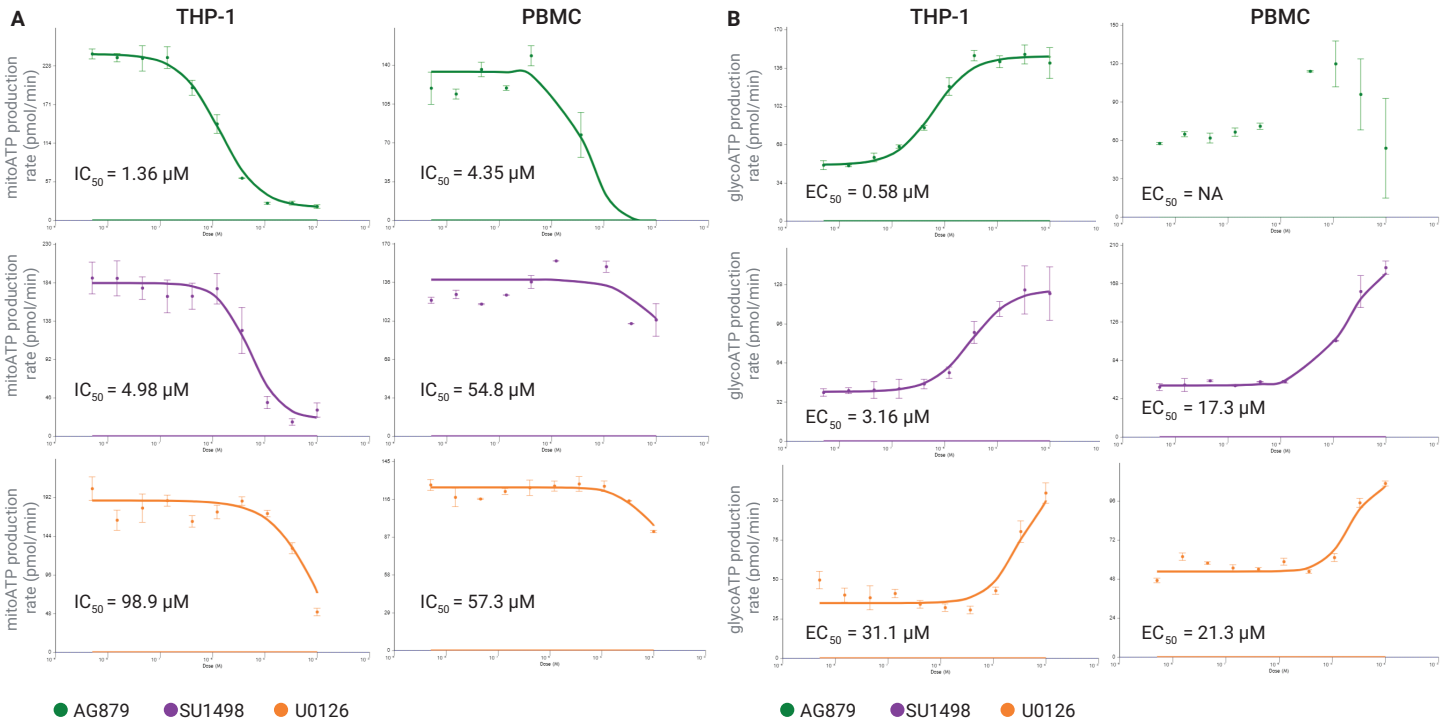

Figure 6. Dose responses of mitoATP rate (A) and glycoATP rate (B) of THP-1 and PBMC to three selected kinase inhibitors. (n = 4, mean ±SD).

Conclusion

The Agilent XF Real-Time ATP rate assay is a simple and robust assay that can identify metabolic target pathways to be investigated during cancer drug discovery. Combined with dedicated analytic software, it provides a direct way to quantitate and compare the metabolic response of cancer cells to chemicals or genetic modification and differentiate mitochondrial and glycolytic energetic metabolism.
This assay is suitable as a starting assay for screening compounds that induce metabolic phenotypic changes in cancer cells without significantly affecting cell viability. In addition, the potency of selected compounds can be evaluated using dose-response assays or subjected to a more comprehensive functional analysis for further detailed pre-clinical investigations.

References

1. Wolpaw, A.; Dang, C. V. Exploiting Metabolic Vulnerabilites of Cancer with Precision and Accuracy. *Trends Cell Biol*. **2018**, *28*, 201–212.
2. Chandel, N. S.; Martinez-Reyes, I. Cancer Metabolism: Looking Forward. *Nat. Rev. Cancer* **2021**, *21*, 669–680.
3. Stine, Z. E. *et al.* Targeting Cancer Metabolism in the Era of Precision Oncology. *Nat. Rev. Drug Discov.* **2022**, *21*, 141–162.
4. Romero, N. *et al.* Quantifying Cellular ATP Production Rate Using Agilent Seahorse XF Technology. *Agilent Technologies white paper*, 5991-9303EN, **2018**.
5. Carling, D. *et al.* AMP-Activated Protein Kinase: New Regulation, New Roles? *Biochem. J*. **2012**, *445*, 11–27.

6. Hardie, D. G., Ross, F. A., Hawley, S. A. AMPK: a Nutrient And Energy Sensor That Maintains Energy Homeostasis. *Nat. Rev. Mol. Cell Biol.* **2012**, *13*, 251–262.
7. Agilent Seahorse XF Real-Time ATP Rate Assay Kit User Guide, 103592-100. *Agilent Technologies*, **2018**.
8. Agilent Seahorse XF Media Selection Guide. *Agilent Technologies*, 5994-7878EN, **2020**.
9. Bravo Seahorse Assay Workbench User Guide. *Agilent Technologies*, 5994-0684EN, **2019**.
10. Bravo Automated Workflow for Seahorse XFe96 Sample Preparation. *Agilent Technologies*, https://www.agilent.com/en/video/bravo-xf-demonstration (accessed 2022-12-16)
11. Boguslawski, G. *et al.* SU1498, an Inhibitor Of Vascular Endothelial Growth Factor Receptor 2, Causes Accumulation of Phosphorylated ERK Kinases and Inhibits Their Activity *In Vivo* and *In Vitro*. *J. Biol. Chem.* **2004**, *279*, 5716–5724.
12. Hao, T.; Rockwell, P. Signaling Through the Vascular Endothelial Growth Factor Receptor VEGFR-2 Protects Hippocampal Neurons from Mitochondrial Dysfunction and Oxidative Stress. *Free Radic. Biol. Med.* **2013**, *63*, 421–431.
13. Kerr, A. H. J. *et al.* An Investigation of the MEK/ERK Inhibitor U0126 in Acute Myeloid Leukemia. *Ann. N. Y. Acad. Sci.* **2003**, *1010*, 86–89.
14. Freeman, M. R. *et al.* Metabolic Perturbation by U0126 Identifies a Role for Glutamine in Resveratrol-Induced Cell Death. *Cancer Biol. Ther.* **2011**, *12*, 966–977.
15. Vera, J. C. *et al.* Direct Inhibition of the Hexose Transporter GLUT1 by Tyrosine Kinase Inhibitors. *Biochemistry* **2001**, *40*, 777–790.

www.agilent.com

RA44944.6254050926

Printed in the USA, January 27, 2023
5994-5651EN

Agilent
Trusted Answers